

Received December 16, 2019, accepted January 6, 2020, date of publication January 13, 2020, date of current version January 21, 2020.

Digital Object Identifier 10.1109/ACCESS.2020.2966275

# A Reliability Assessment Approach for Electric Power Systems Considering Wind Power Uncertainty

XYUN YANG<sup>1,2</sup>, YUWEI YANG<sup>1</sup>, YUQI LIU<sup>1,3</sup>, AND ZIQI DENG<sup>1</sup>

<sup>1</sup>School of Control and Computer Engineering, North China Electric Power University, Beijing 102206, China

<sup>2</sup>Key Laboratory of Condition Monitoring and Control for Power Plant Equipment of Ministry of Education, North China Electric Power University, Beijing 102206, China

<sup>3</sup>Laboratory of Networked Control Systems, Shenyang Institute of Automation, Chinese Academy of Sciences, Shenyang 110016, China

Corresponding author: Yuwei Yang (18511791255@163.com)

This work was supported in part by the National Natural Science Foundation of China under Grant 51677067, and in part by the Fundamental Research Funds for the Central Universities under Grant 2018MS27.

**ABSTRACT** The intermittence and uncertainty of wind power pose challenges to large-scale wind power grid integration. The study of wind power uncertainty is becoming increasingly important for power system planning and operation. This paper proposes a wind power probabilistic interval prediction model, and a novel reliability assessment approach is presented for electrical power systems. First, the unknown parameters estimation of the autoregressive integrated moving average (ARIMA) prediction model is based on the Markov chain Monte Carlo (MCMC)-based Bayesian estimation method to improve the quality of statistical inference. Then, a quantum genetic algorithm is used to segment the power to determine the best output for each power segment weight and calculate the probabilistic prediction interval of wind power. Finally, reliability assessment by the sequential Monte Carlo simulation is presented combining with the probabilistic prediction interval of wind power on IEEE-RTS79 reliability test system. The simulation results that proposed variation range of reliability assessment indices consider the uncertain scenario of wind power and has guiding significance for power generation scheduling. Compared with genetic algorithm and particle swarm optimization algorithm, it is proved that the proposed prediction interval model has better prediction interval coverage probability index and interval average bandwidth index.

**INDEX TERMS** Bayesian estimation, interval prediction, reliability index, sequential Monte Carlo method, wind power.

## I. INTRODUCTION

Wind power has become one of the most popular renewable energy sources in the world, as it reduces the use of fossil fuels and saves greenhouse gas emission costs. However, the intermittence and volatility of wind power has restricted large-scale integration of wind turbines into power systems and poses new uncertainties and challenges to power system reliability [1]. It is thus necessary to assess the impact of wind power on power system reliability.

High-precision wind power forecasting is an effective means of alleviating the negative influence of wind power generation on power systems [2]–[4]. Many physical and statistical prediction methods have been proposed in

The associate editor coordinating the review of this manuscript and approving it for publication was Junjian Qi<sup>1,3</sup>.

recent years. Physical models use numerical weather prediction to predict wind speed and then input the data into wind power output models to obtain output power [5]. Common statistical forecasting methods include the time series method [6], [7], artificial neural network method [8]–[10], and support vector machine (SVM) [11]. The main focus of these methods is to decrease the point forecast errors of wind power by introducing new models. In [12], quantiles were created using a nonparametric approach to forecast wind power. Although this method does not make any assumptions about the forecast error distribution, it suffers from a linear structure, which can compromise forecasting accuracy. In [13], an improved Elman neural network model was developed for a multi-target satin cypress optimization algorithm. Literature [14] proposed a new prediction method by combining stacked auto-encoders (SAE) and the back

propagation (BP) algorithms. In [15], a new L-BFGS optimization method, based on the Riemannian manifold, is used for GMM parameter estimation. Based on actual wind power forecast error data, the suitability of the model and the new optimization algorithm was verified. However, even with the best predictive tools, prediction error could not be completely eliminated. In recent years, the study of probability interval prediction that reflects wind power uncertainty information has received increasing attention [16]. In [17], a probabilistic interval prediction model based on quantile regression averaging and variational mode decomposition-based hybrid models was presented to quantify potential risks of wind power series. In [18], a prediction model was established through a kernel extreme learning machine. A key issue in these methods is how to select reasonable trained data to obtain a high-precision intelligent model that approximates the nonlinear relationship between input and output variables. To this point, studies have obtained wind power prediction intervals either by analyzing the error characteristics of point prediction or using an intelligent model; however, such models often neglect to consider probabilistic information related to wind speed or power data in historic operation data. Yet probabilistic interval prediction provides more information compared with point prediction, and high-accuracy interval prediction can facilitate risk assessment related to wind power in power system planning and scheduling. In our work, to study reliability assessment for the uncertainty of wind power integrated into the grid, we first build a wind power probabilistic interval prediction model that combines an autoregressive integrated moving average (ARIMA) model based on a Markov chain Monte Carlo (MCMC)-based Bayesian estimation with optimized interval weights using a quantum genetic algorithm (QGA). Different from prior research, the advantage of the proposed interval predication model is that MCMC-based Bayesian estimation uses probabilistic information to estimate unknown parameters in the ARIMA model to improve the quality of statistical inference. Furthermore, without an assumed error distribution, the QGA can search each power range segmentally to determine its optimal output weight in the interval model and then calculate the upper and lower bounds of the wind power prediction interval. Thus, a high-quality interval forecasting model of wind power can be achieved.

As wind power is integrated into the grid on a large scale, the uncertainty of wind power output will exert an increasingly large impact on the operational reliability of the power system. Effectively and accurately analyzing the impact of a wind-farm-integrated grid on power generation reliability can provide a theoretical basis for the effective use of wind power. Several scholars have studied the reliability of wind farm power systems. Common approaches include analytical methods and simulation methods [19]. Literature [20] used a Monte Carlo sampling method for stochastic production simulation to evaluate the effects of wind farms on power system production and operation. In [21], a non-sequential Monte Carlo simulation method was used to analyze the

equivalent capacity of wind farms considering the wind speed correlation at different locations, and the effects of different degrees of correlation on system reliability were studied. Literature [22] presents a new method for load modeling in power system reliability evaluation. The method combines the fuzzy model for the peak load with a probability distribution for a load curve, whereas system component outages can still be modeled using traditional Monte Carlo or enumeration techniques. Literature [23] described a proposed coupled extreme frame weather event to cascade a failure simulation model. Then, a custom sequential Monte Carlo simulation scheme was developed to quantify extreme weather events affecting power transmission. However, most studies have focused on the impact of wind power on power system reliability; few discussions have considered the fluctuation range of wind power uncertainty.

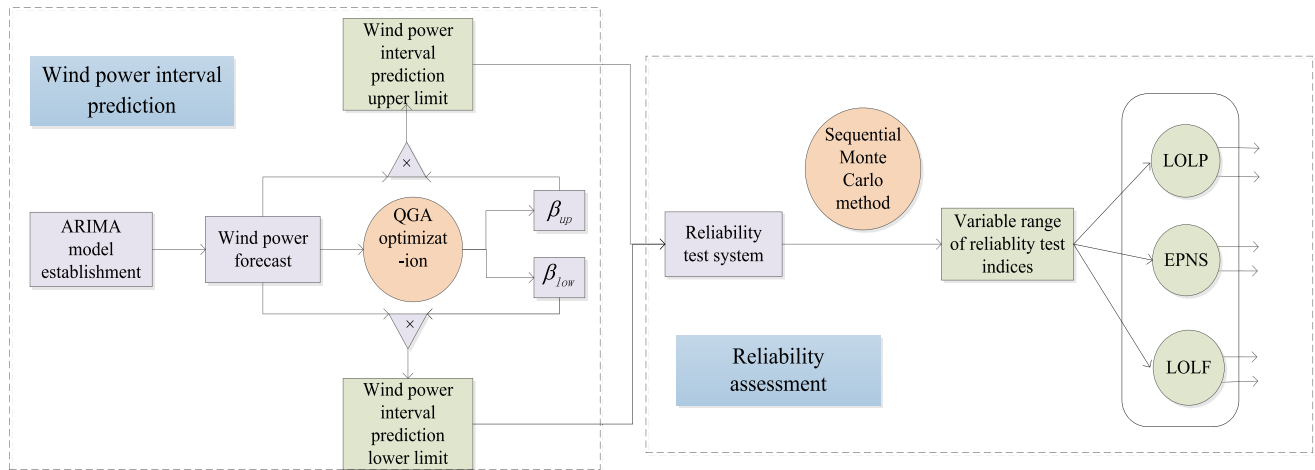
To address this research gap, our paper aims to outline a reliability assessment approach for electrical power systems considering of wind power uncertainty based on a probabilistic interval prediction model. The contributions of this paper mainly include two parts: One is that the variation ranges of reliability indices by sequential Monte Carlo methods are obtained for the first time for a power system under an IEEE-RTS79 reliability test system, which is combined with wind power probabilistic interval prediction model. The variation range of three system reliability indices can be obtained: loss of load probability (LOLP), expected power not supply (EPNS), and loss of load frequency (LOLF). These reliability indices thus carry reference significance for power system decision makers. The other contribution is wind power interval prediction model using ARIMA based on MCMC-based Bayesian estimation and interval weight parameters optimized via QGA. Taken interval coverage and interval average bandwidth are selected as evaluation criteria, compared with the genetic algorithm (GA) and particle swarm optimization (PSO) algorithm, our simulation results show that the proposed prediction interval model has superior prediction accuracy and general accuracy.

The rest of this paper is organized as follows. In Section 2, the overall flow chart of reliability assessment approach is given. In Section 3, a wind power interval prediction model based on QGA-MCMC-ARIMA is described. The reliability index calculation model is presented in Section 4, and numerical studies of the proposed approach are demonstrated in Section 5. Finally, conclusions are drawn in Section 6.

## II. ASSESSMENT FRAMEWORK

This paper aims to outline a reliability assessment approach for electrical power systems considering of wind power uncertainty based on a probabilistic interval prediction model. It is mainly divided into two parts.

First, the method based on MCMC Bayesian estimation ARIMA model combining with upper and lower weight of interval prediction model by QGA optimization is used to predict wind power interval. To compare the effectiveness of the QGA-MCMC-ARIMA optimization model proposed in

**FIGURE 1.** Overall flow chart.

this paper, GA-MCMC-ARIMA and PSO-MCMC-ARIMA were used to predict wind power range, and the predict interval coverage probability and the prediction interval average width were compared under different confidence levels.

Second, On the basis of this interval prediction model, an IEEE-RTS79 reliability test system is built, and the variation ranges of reliability indices are obtained for a power system integrating wind power using sequential Monte Carlo methods. The power system reliability index selects the Loss of Load Probability (LOLP, representing the probability of a power outage event in the system); Loss of Load Frequency (LOLF, indicating the number of times the system has a load shedding failure per unit time), and the Expected Power Not Supply (EPNS).

Fig. 1 presents the Overall flow chart.

### III. WIND POWER INTERVAL PREDICTION MODEL BASED ON QGA-MCMC-ARIMA

#### A. BAYESIAN ESTIMATION OF ARIMA MODEL PARAMETERS

The ARMA(p,q) model, specifically the autoregressive moving average, is a common power prediction method. Wind power is often unstable due to its volatility and intermittent nature. The ARIMA(p,d,q) model, specifically the autoregressive integrated moving average model, is an extension of the ARMA(p,q) model. It converts the non-stationary time series into a stationary time series using the d-order difference method, and then builds the ARMA(p,q) model:

$$y'_t = \sum_{i=1}^p \varphi_i y'_{t-i} + \sum_{j=1}^q \theta_j \varepsilon_{t-j} + \varepsilon_t \quad (1)$$

In (1),  $p$  and  $q$  are each non-negative integers representing the order of the autoregressive and moving average terms in the model;  $\varphi_i$  is the coefficient of the  $i$ -th autoregressive term;  $\theta_j$  is the coefficient of the  $j$ -th moving average; and  $\varepsilon_t$  is the residual term, which is an independent and identically distributed random variable, that obeys a normal

distribution with a mean of 0. In this paper, the ARIMA model is selected for wind power prediction. The stationary sequence is obtained by the difference, and then the ARMA model is established for the new stationary sequence.

In traditional classical statistical theory, the unknown parameters  $\varphi_i$  and  $\theta_j$  in ARIMA are constant, whereas the Bayesian parameter estimation considers unknown parameters  $\varphi_i$  and  $\theta_j$  in ARIMA as random variables that can be described by the probability distribution. This probability distribution is called the prior distribution of unknown parameters. Compared with the conventional estimation method, Bayesian estimation makes full use of prior distribution information from the sample information model parameters and incorporates it into statistical inference. The estimator has a smaller variance and square difference, which improves the statistical inference quality. The core idea of Bayesian estimation is to obtain the Bayesian posterior distribution of unknown parameters via the Bayesian theorem and then use the posterior distribution to estimate model parameters.

Assume that  $e_t \sim N(0, \tau^{-1})$  is the initial value of a given time series,  $\{y, t \in T\}$  is a time series, and  $y_1, y_2, \dots, y_n$  is the sequence observation. The ARMA (p, q) model is  $\varphi(L)y_t = \theta(L)\varepsilon_t$ , where the error term  $\varepsilon_t \sim N(0, \sigma^2)$ . Then, the likelihood function of the ARMA model is

$$\begin{aligned} L(y | \bar{y}, \varphi, \theta, \tilde{\varepsilon}) &= \prod_{t=1}^n \left(2\pi\sigma^2\right)^{-\frac{1}{2}} \exp\left(-\frac{\varepsilon_t^2}{2\sigma^2}\right) \\ &= \left(2\pi\sigma^2\right)^{-\frac{n}{2}} \exp\left(-\frac{1}{2\sigma^2} \sum_{t=1}^n \varepsilon_t^2\right) \end{aligned} \quad (2)$$

$$\bar{y} = (y_1, y_2, \dots, y_p)^T$$

$$\text{where } y = (y_1, y_2, \dots, y_n)^T, \quad \tilde{\varepsilon} = (\varepsilon_1, \varepsilon_2, \dots, \varepsilon_q)^T, \quad \varphi = (\varphi_1, \varphi_2, \dots, \varphi_p)^T, \quad \theta = (\theta_1, \theta_2, \dots, \theta_q)^T$$

Assuming the parameter  $\varphi_i$  ( $i = 1, 2, \dots, p$ ), the parameter  $\theta_j$  ( $j = 1, 2, \dots, q$ ) obeys the uniform distribution, that is,  $\pi_{\varphi_i}(\varphi_i) \propto 1, i = 1, 2, \dots, p$ ;  $\pi_{\theta_j}(\theta_j) \propto 1, j = 1, 2, \dots, q$ ,

Then, using Bayes' theorem, the posterior distribution density functions of the parameters  $\varphi_i$  and  $\theta_j$  are

$$P_{\varphi_i}(\varphi_i|X, \tilde{X}, \varphi_{-i}, \theta, \sigma^2, \tilde{\varepsilon}) \propto L(X|\tilde{X}, \varphi, \theta, \sigma^2, \tilde{\varepsilon}) \pi_{\varphi_i}(\varphi_i) \\ \propto \exp\left\{-\frac{1}{2\sigma^2} \sum_{t=1}^n \varepsilon_t^2\right\} \quad (3)$$

$$P_{\theta_i}(\theta_i|X, \tilde{X}, \varphi, \theta_{-j}, \sigma^2, \tilde{\varepsilon}) \propto L(X|\tilde{X}, \varphi, \theta, \sigma^2, \tilde{\varepsilon}) \pi_{\theta_i}(\theta_i) \\ \propto \exp\left\{-\frac{1}{2\sigma^2} \sum_{t=1}^n \varepsilon_t^2\right\} \quad (4)$$

Here, we use the MCMC Bayesian method based on Gibbs sampling to estimate the parameters of the ARIMA model.

## B. PARAMETER ESTIMATION BASED ON MCMC BAYESIAN METHOD

### 1) BASIC IDEA OF THE MCMC METHOD

In Bayesian calculations, we typically use integral methods that require analysis or numerical approximation, including sample-based Monte Carlo sampling (e.g., important sampling, stratified sampling, and associated sampling), to sample from the posterior distribution to estimate parameters of interest. However, it is often difficult to generate samples directly from an arbitrary high-dimensional joint distribution, which limits the sample-based method. The MCMC method is a simple and effective Bayesian calculation method developed recently. It applies the Markov chain in the stochastic process to the Monte Carlo simulation to achieve dynamic simulation (the i.e., the sampling distribution changes as the simulation proceeds).

The sequence  $\{X^{(0)}, X^{(1)} \dots, X^{(k+1)}\}$  is derived from the conditional distribution of  $\{X^{(k+1)}|X^{(k)}\}$ , where  $X^{(0)}$  represents an initial condition, and  $X^{(0)}, X^{(1)}, X^{(2)} \dots, X^{(k+1)}$  is a Markov chain.

When  $k \rightarrow \infty$ ,  $X^{(k)}$  is independent of the initial value, and its density (distribution) approaches a stationary distribution, which is  $p^*(\cdot)$ . That is, as  $k$  increases, the random vector in the Markov chain will converge to a Markov sequence with a common density  $p^*(\cdot)$ . At this time, the Markov chain is said to converge; in the period before convergence (as in the previous  $M$  sampling), the density distribution of each state is not the stationary distribution. Therefore, the first  $M$  samples should be removed when estimating  $E[f(x)]$ , such that the estimated results are obtained after  $n-M$  samples:

$$E[f(x)] = \frac{1}{n-M} \sum_{k=M+1}^n f(X_k) \quad (5)$$

Equation (1) is the famous traversal average in the random process. The variance of the estimate is

$$\hat{V}[E(f)] = V(f)/n \quad (6)$$

The estimated value of  $V(f)$  is

$$\hat{V}(f) = \frac{1}{n-1} \sum_{i=1}^n \left[ f(x_i) - \hat{E}(f) \right]^2 \quad (7)$$

From the above analysis of MCMC theory, the main idea of MCMC is to construct a Markov chain with a stable distribution of  $p(x)$ . It is simple to construct such a Markov chain; the most commonly used algorithms are Metropolis-Hastings (M-H) and the Gibbs sampler [24]. Due to the advantages of Gibbs sampling in terms of high-dimensional features and sampling paths, Gibbs sampler is used in this calculation to generate the Markov chain required for MCMC simulation.

### 2) MCMC BAYESIAN METHOD FOR ESTIMATING ARIMA PARAMETERS

Here, we use the MCMC Bayesian method based on Gibbs sampling to estimate ARIMA model parameters. The steps are as follows:

*Step 1:* Given the initial value  $\varphi_1^{(0)}, \varphi_2^{(0)}, \dots, \varphi_p^{(0)}; \theta_1^{(0)}, \dots, \theta_q^{(0)}$  of  $\varphi, \theta$ , let  $a=1$ .

*Step 2:* Extract the parameter  $\varphi_i(i=1, 2, \dots, p)$  from

$$P_{\varphi_i} \left( \begin{array}{c} \theta_i|X, \tilde{X}, \varphi^{(a-1)}, \theta_1^{(a-1)}, \dots, \theta_{j-1}^{(a-1)}, \theta_{j+1}^{(a-1)}, \\ \dots, \theta_q^{(a-1)}, \sigma^{2(a-1)}, \tilde{\varepsilon} \end{array} \right).$$

*Step 3:* Extract the parameter  $\theta_i(i=1, 2, \dots, q)$  from

$$P_{\theta_i} \left( \begin{array}{c} \varphi_i|X, \tilde{X}, \varphi_1^{(a-1)}, \dots, \varphi_{i-1}^{(a-1)}, \varphi_{i+1}^{(a-1)}, \\ \dots, \varphi_p^{(a-1)}, \theta^{(a-1)}, \sigma^{2(a-1)}, \tilde{\varepsilon} \end{array} \right).$$

*Step 4:* Let  $a = a + 1$  and return to Step 2.

Steps 2 through 5 are repeated  $M$  times until Markov converges and the first  $N$  iterations are rounded off to eliminate the effect of the initial value on the estimate.

## C. BASED ON QGA SEGMENTATION OPTIMIZATION POWER INTERVAL PREDICTION

After the ARIMA model obtains the wind power point prediction model, the value of the point prediction is multiplied by  $\beta_1$  and  $\beta_2$ , and the obtained results are the upper and lower limits of the interval prediction, respectively.  $\beta_1$  is upper limit weight of interval prediction model, and  $\beta_2$  is the lower limit weight of interval prediction, which  $\beta_1$  and  $\beta_2$  are obtained via QGA segmentation optimization. Fig. 2 presents a schematic diagram of the interval prediction model.

### 1) OPTIMIZING THE OBJECTIVE FUNCTION

Evaluating the accuracy of the prediction interval output by the prediction model involves two aspects: reliability and accuracy. Reliability is expressed as the probability that the actual observation falls within the prediction interval; this value should be as large as possible to make the prediction more accurate. Accuracy is used to measure the interval width; this value should be as small as possible so the prediction width is as narrow as possible. However, the two are contradictory. In this paper, constructing an objective function should consider the above two aspects and define the comprehensive optimization objective function  $F$  as follows:

$$(min) F = \sum_{\beta}^n [\gamma_i |PICE_t^{\alpha}| + \varphi_i |PINAW_t^{\alpha}|] \quad (8)$$

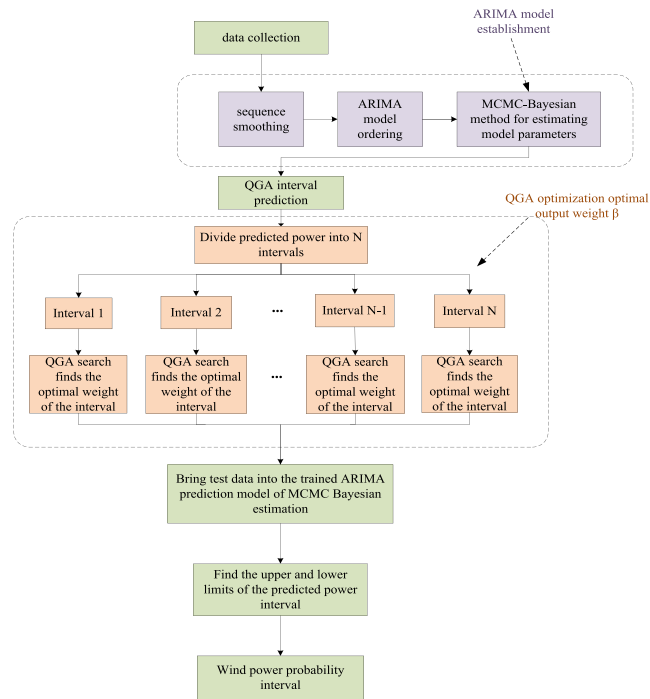


**FIGURE 2.** Estimation of ARIMA interval prediction model based on MCMC Bayesian method combined with QGA.

where  $PICE = |PINC - PICP|$ . PINC is the PI nominal confidence; PICP is the prediction interval coverage probability, which is a reliability indicator for evaluating the prediction interval.  $\alpha$  means to the confidence level. As shown in (9), this index reflects the probability that the actual observation  $t_i$  falls within the upper and lower limits of the prediction interval:

$$PICP = \frac{1}{N_t} \sum_{i=1}^{N_t} \kappa^\alpha \quad (9)$$

where  $N_t$  is the number of predicted samples.  $\kappa^\alpha$  is the Boolean quantity; if the predicted target value  $t_i$  is included in the upper and lower limits of the interval prediction, then  $\kappa^\alpha = 1$ , and  $\kappa^\alpha = 0$  otherwise. The significance of this value in the objective function is that in actual predictions, to obtain a valid prediction interval, the PICP should be as close as possible to the preset nominal confidence level of the PINC.

The second PINAW in the objective function is the prediction interval average width, reflecting the clarity of prediction, as shown in (10). This equation avoids the risk of the prediction interval being too wide due to the pure pursuit of reliability. In this case, the effective prediction value uncertainty information could not be obtained, and the decision value would be lost:

$$PINAW = \frac{1}{N_t} \sum_{i=1}^{N_t} [U_t^\alpha(x_i) - L_t^\alpha(x_i)] \quad (10)$$

where  $\gamma_i$  and  $\varphi_i$  are the weighting coefficients for the prediction target coverage deviation and the prediction interval average bandwidth, and these coefficients are adjusted to control

the influence ratios of different criteria on the optimization effect.  $|\cdot|$  is used to obtain the absolute values for PICE and PINAW, respectively.

## 2) QGA SEGMENTATION OPTIMIZATION OPTIMAL PREDICTION WEIGHT $\beta$

The output weights of prediction models of different power segments are unique. If the same output weight is used, the accuracy of the prediction interval will be reduced. Therefore, the power interval is divided and QGA is applied in this paper to identify the optimal output weight of each power segment.

QGA merged as a research field in the late 1990s, mainly introducing concepts related to quantum computing into GAs. In QGA, a qubit-based coding scheme is used, wherein a quantum bit is defined by a pair of complex numbers, and a system with  $m$  qubits can be described as

$$\begin{vmatrix} \alpha_1 & \alpha_2 & \alpha_3 & \cdots & \alpha_m \\ \lambda_1 & \lambda_2 & \lambda_3 & \cdots & \lambda_m \end{vmatrix}$$

where  $|\alpha_i|^2 + |\lambda_i|^2 = 1 \quad (i = 1, 2, \dots, m)$

A qubit is a two-state quantum system that acts as a physical medium for an information storage unit. It is a unit vector defined in a two-dimensional vector space that can be superposed in two quantum states simultaneously, such as  $|\delta\rangle = \alpha|0\rangle + \lambda|1\rangle$ , where 0 and 1 represent the spin-down state and spin-up state, respectively.  $|\delta\rangle$  is a representation of a quantum state, where  $\alpha$  and  $\lambda$  are two complex numbers called probability pairs, and their respective squares can be considered the probability that the quantum is in a spin-down state or spin-up state.

QGA also uses the operation of quantum revolving door to realize chromosome updates. The algorithm thus has the ability to develop and explore, to obtain the optimal solution of the target. Commonly used quantum gate transformation matrices have XOR gate-controlled XOR gate revolving gates and Hadamard transform gates. In the quantum genetic iteration of this paper, the population is updated with the following quantum revolving gate:

$$\begin{vmatrix} \alpha'_i \\ \lambda'_i \end{vmatrix} = \begin{vmatrix} \cos \theta_i & -\sin \theta_i \\ \sin \theta_i & \cos \theta_i \end{vmatrix} \begin{vmatrix} \alpha_i \\ \lambda_i \end{vmatrix}$$

where:  $\alpha_i$  and  $\lambda_i$  denote the  $i$ -th qubit in the chromosome, and  $\theta_i$  is the rotation angle.

The quantum genetic algorithm combines quantum computing with genetic algorithms, and introduces quantum coding and quantum revolving doors to increase the possibility of chromosomal changes. This paper chooses the QGA algorithm to optimize the output weight  $\beta$ . The optimization process is as follows:

- (1) Take the initial population  $Q(t)$  with a population size of  $N$ .
- (2) Perform a measurement on each individual of the initial population to obtain a state  $P(t)$ . When measuring, select 0 or 1 on the corresponding gene position according to the quantum bit probability. The specific method is as follows:

randomly generate a [0, 1] number, and if it is greater than or equal to the value of the probability amplitude, then the measurement result is taken as 1; otherwise, the results is taken as 0 (and vice versa).

(3) Record the fitness of each state along with the best individual and its fitness value.

(4) Use hybridization, variation, and quantum revolving gates to update individual populations and measure individual population status.

(5) Record the best individual and its fitness value. If the value is greater than the current optimal value, then update the optimal value; otherwise, retain the current value.

(6) If the end condition (i.e., a sufficiently good solution or maximum number of iterations) is reached, then optimization ends. The group optimum at this time is the optimal output weight  $\beta$ ; otherwise, return to Step (2).

(7) Output data and terminate.

#### D. SPECIFIC STEPS OF WIND POWER INTERVAL PREDICTION MODEL

STEP 1 using MCMC Bayesian estimation parameters of ARIMA model, obtains wind power point prediction value from ARIMA model;

STEP 2 initializes QGA parameters, including setting the population number, initial position, individual extremum and total extremum;

STEP 3 divides the wind power into different power segment and uses QGA to optimize output weight  $\beta_1$  and  $\beta_2$  of prediction interval in different power segments. According to the objective function, the fitness and global value of each particle are calculated in each iteration. Finally, the optimal output weight  $\beta_1$  and  $\beta_2$  are obtained;

STEP 4 Multiply the point prediction values output by the ARIMA model by  $\beta_1$  and  $\beta_2$ , respectively, to obtain the upper and lower limits of the wind power prediction interval.

### IV. RELIABILITY INDEX CALCULATION MODEL

#### A. SEQUENTIAL MONTE CARLO METHOD

In this study, the sequential Monte Carlo method was used to calculate the reliability index of the system. Monte Carlo is a numerical calculation method based on probability and statistics and is widely used in power system risk assessment [25]. The sequential Monte Carlo method considers the continuity of the system on the basis of the non-sequential Monte Carlo method, samples the working state duration of all components, forms the timing state of the system, and performs reliability analysis [26]. Compared with the non-sequential Monte Carlo method, the advantage of the latter method lies in its clear physical meaning, low algorithm complexity, and shortcomings of slow convergence, rendering it suitable for advanced grid reliability planning.

The sequential Monte Carlo simulation flow chart for the power system is illustrated in Fig. 3. The state of components in the transmission system adopts a two-state model, as shown in Fig. 4.

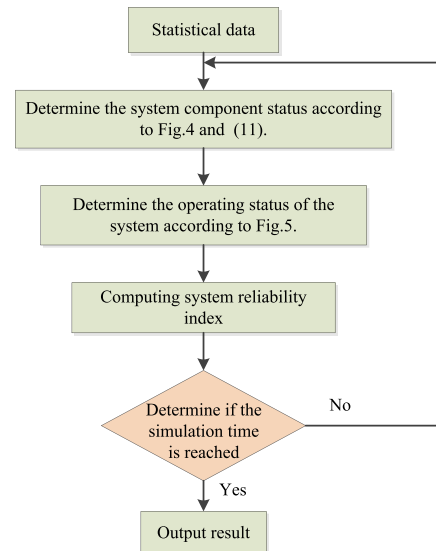


**FIGURE 3.** Sequential Monte Carlo simulation flow chart.

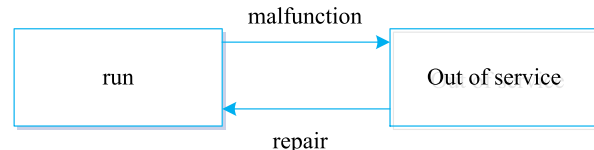


**FIGURE 4.** State transition of state components.

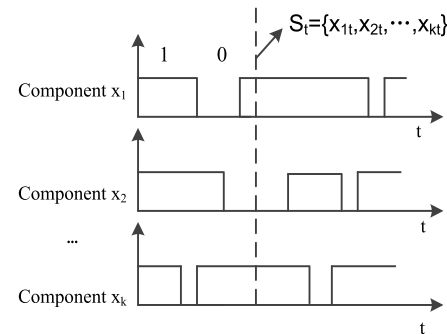


**FIGURE 5.** System operation status determination.

The trouble-free running time  $T_{TTF}$  of the power generation system components and estimated fault repair time  $T_{TTR}$  are calculated as

$$\begin{cases} T_{TTF} = -T_{MTTF} \times \ln(1 - R_1) \\ T_{TTR} = -T_{MTTR} \times \ln(1 - R_2) \end{cases} \quad (11)$$

where  $R_1$  and  $R_2$  are random numbers between [0,1];  $T_{MTTF}$  and  $T_{MTTR}$  are the average fault-free working time and average repair time of the component, respectively, and are the reciprocal of the failure rate  $\lambda$  and repair rate  $\mu$ ;  $T_{TTF}$  and  $T_{TTR}$  are the fault-free running time and fault repair time of the original power generation system, respectively.

Assuming that the system consists of  $k$  components, the operating state of each component is determined by (11). Then the system operating state  $S_t$  at time  $t$  is determined by the operating state  $X_{kt}$  of each component, as shown in Fig. 5,

where 1 represents component operation and 0 represents component failure.

### B. SYSTEM RELIABILITY INDEX

#### CALCULATION PROCEDURE

Before the system is newly connected to the wind farm, we must analyze the degree of wind farm reliability. It is difficult to accurately evaluate the wind farm due to its strong randomness. In this paper, based on the interval prediction model with wind power uncertainty information established above, a simple and feasible calculation method for evaluating the degree of influence of a wind power plant on the system is proposed. The specific reliability interval calculation steps are as follows:

- 1) Build a reliability test system IEEE-RTS79; specific parameters are detailed in the [27]. The power system reliability index selection includes LOLP, indicating the probability of a power outage event in the system (dimensionless); EPNS (MW); and LOLF, indicating the number of times the system has a load shedding failure per unit time (sub/year). The calculation formula is

$$\begin{aligned} LOLP &= \frac{1}{T} \sum_{i=1}^N [F_{LOLP}(X_i) \cdot t_i] \\ EPNS &= \frac{1}{T} \sum_{i=1}^N [F_{EPNS}(X_i) \cdot t_i] \\ LOLF &= \frac{8760}{T} \cdot C_L \end{aligned} \quad (12)$$

where  $F_{LOLP}(X_i)$  and  $F_{EPNS}(X_i)$  are test functions corresponding to LOLP and EPNS, respectively,  $F_{LOLP}(X_i)$  is calculated using (13), and  $F_{EPNS}(X_i)$  is the total active load cutoff power of the system in random state  $X_i$ ;  $C_L$  is the number of shear loads during the simulation time;  $T$  is the total simulation time for the system; and  $t_i$  is the duration of the system state  $X_i$ .

$F_{LOLP}(X_i)$

$$= \begin{cases} 0 & \text{The system has a load shedding in state } X_i \\ 1 & \text{The system has no load shedding in state } X_i \end{cases} \quad (13)$$

- 2) The wind farm is connected to the system, and the access scheme refers to the distributed access method of [28];

- 3) According to the wind farm power interval prediction model, it is assumed that the wind farm output power is taken as the upper or lower limit of the interval prediction model, respectively, and the reliability result is obtained via simulation to determine the reliability interval of the wind farm in access mode.

### V. CASE ANALYSIS

Taking a wind farm in the northwest China as an example, the rated power of wind turbine is 2MW and the time resolution is 15 min. Using wind power data collected from the site in 2014, the feasibility of this method is verified via simulation, and the reliability index is obtained.

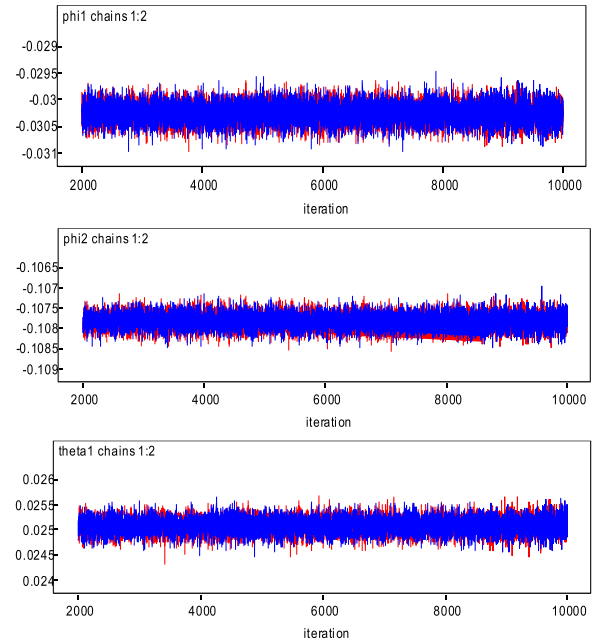


**FIGURE 6.** Markov chain trajectory of ARIMA model parameters  $\varphi$  and  $\theta$ .

### A. WIND POWER INTERVAL PREDICTION SIMULATION RESULTS

#### 1) ARIMA MODEL ESTABLISHMENT

Wind power is often unstable due to its volatility and intermittent nature. Therefore, the wind power time series  $\{y_t\}$  must be tested for smoothing before the model is built.

As the sequence  $\{y_t\}$  is non-stationary, the original sequence  $\{y_t\}$  is smoothed by the first-order difference method to obtain a new time series  $\{y'_t\}$ , such that

$$y'_t = y_{t+1} - y_t \quad (14)$$

We then verify that the new sequence  $\{y'_t\}$  is stationary.

From the smoothing process of this sequence, the difference order  $d = 1$ ; thus, the ARMA (p, q) model is built for the time series after the difference. The group with the smallest Akaike information criterion (AIC) value is selected according to the autocorrelation and partial autocorrelation coefficient map of the sequence, as well as the order rule and the AIC. According to the AIC, and considering the significance of parameters, the ARMA (2,1) model is finally selected to fit the time series  $\{y'_t\}$ . Then, the time series model to be fitted is

$$y'_t = \varphi_1 \cdot y'_{t-1} + \varphi_2 \cdot y'_{t-2} + \theta_1 \cdot e_{t-1} + e_t \quad (15)$$

Therefore, the original time series  $\{y_t\}$  can be expressed as

$$y_t = (1 + \varphi_1) \cdot y_{t-1} + (\varphi_2 - \varphi_1) \cdot y_{t-2} - \varphi_2 \cdot y_{t-3} + e_t + \theta_1 \cdot e_{t-1} \quad (16)$$

In the following, we use the MCMC Bayesian method based on Gibbs sampling to estimate the parameters of the ARIMA model and provide the initial values of the two sets of ARIMA model parameters in the sampling process. Fig. 6 shows the Markov chain trajectory constructed after

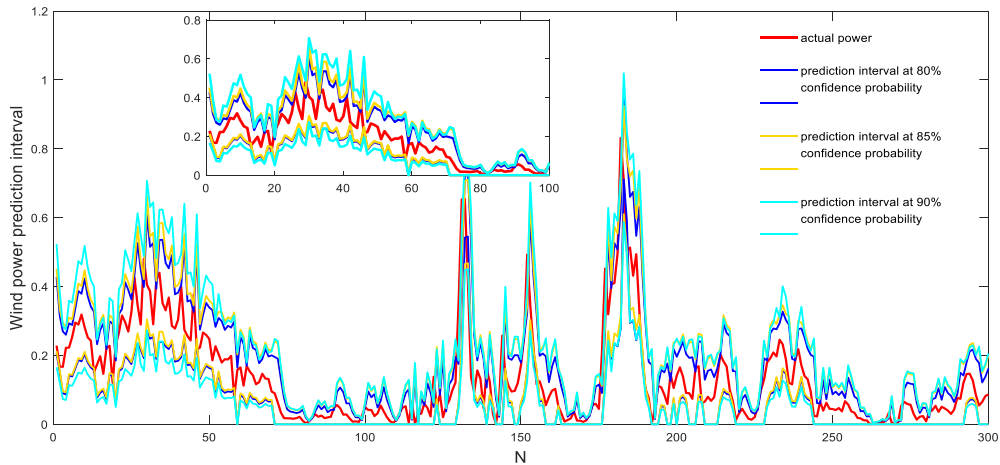


**FIGURE 7.** Prediction interval at 80%, 85%, and 90% confidence levels.

**TABLE 1.** Model parameter estimates.

Parameter	Mean	Standard deviation	Median
$\varphi_1$	-0.03027	$1.911 \times 10^{-4}$	-0.03064
$\varphi_2$	-0.1078	$1.918 \times 10^{-4}$	-0.1082
$\theta_1$	0.02508	$1.587 \times 10^{-4}$	0.02476

parameters  $\varphi$  and  $\theta$  are iterated 10,000 times and 2000 iteration initializations are discarded.

Fig. 6 indicates that the two Markov chains tend to coincide, suggesting that the Markov chain formed after Gibbs sampling was convergent, and the Bayesian estimation of parameters  $\varphi$  and  $\theta$  could be calculated accordingly. Results are listed in Table 1.

We chose the mean as the estimate of the  $\varphi$  and  $\theta$  parameters, after which the ARIMA (2,1,1) model of the original time series  $\{y_t\}$  can be expressed as

$$y_t = 0.96973 \cdot y_{t-1} - 0.07753 \cdot y_{t-2} + 0.1078 \\ \cdot y_{t-3} + e_t + 0.02508 \cdot e_{t-1} \quad (17)$$

Bayesian statistical inference is based on the probability information of historical data, which makes full use of prior distribution information from the sample information model parameters and adds this information to the statistical inference. The estimator thus has smaller variance and square difference, which improves the quality of statistical inference.

## 2) INTERVAL PREDICTION SIMULATION RESULTS AND COMPARISON

Usually, in practical applications, consistently high credibility is ensured to guarantee the safety of normal work. The power system operation must always have a higher level of confidence to obtain more accurate information; therefore, the confidence levels selected in this paper are 80%, 85%, and 90%. The power interval is divided into  $N = 5$ ,  $\gamma_i = 10000$ ,  $\varphi_i = 1$ . Fig. 7 shows the wind farm power interval using the QGA-MCMC-ARIMA prediction model proposed

**TABLE 2.** Optimal output weights for different power segments.

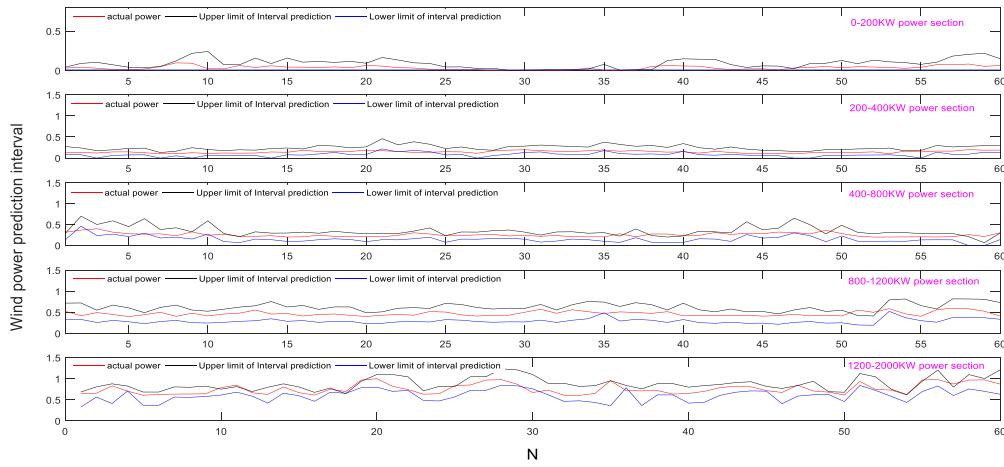
N	$\beta_1$	$\beta_2$
1	2.5015	0
2	1.6315	0.5327
3	1.4066	0.6618
4	1.3773	0.6334
5	1.1408	0.7517

in this paper at 80%, 85%, and 90% confidence levels for 300 consecutive points in November.

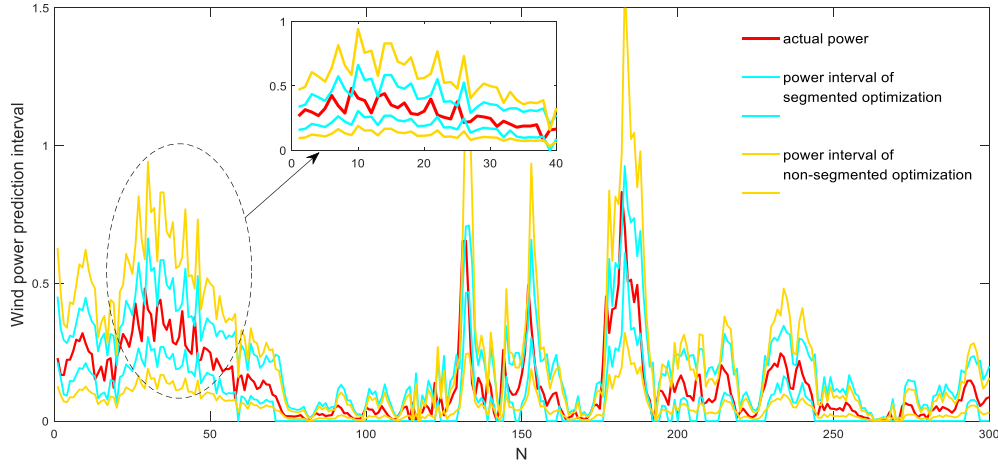
Fig. 7 reveals the following: 1) the wind power probability interval obtained when using the QGA to optimize the output weight of the MCMC-ARIMA prediction model reflects the coverage probability of the actual power value. This approach is also guaranteed to track changes in the wind power time series. 2) The width of the confidence interval increased as the confidence increased; the greater the confidence interval, the greater the probability of including the actual power value, which is consistent with theoretical estimation.

Table 2 shows the output weights for each power segment corresponding to the MCMC-ARIMA prediction model after segmentation optimization at the 85% confidence level. The optimal output weights of various power segments differed. Segmentation optimization should be used to identify the optimal output weight of each power segment, thereby improving the accuracy of the prediction interval. Fig. 8 shows the results of interval prediction for different power segments.

Fig. 9 shows that, under the same confidence level, the comparison between the prediction result of the segmentation optimization prediction model and that of non-segmented optimization is narrow but ensures tracking of wind power time series changes. The upper and lower limits of the interval represent more accurate forecasts and can better guide decision makers.



**FIGURE 8.** Results of prediction interval for using different numbers of power segments.



**FIGURE 9.** Prediction interval of segmented optimization and non-segmented optimization at 85% confidence level.

In order to verify the effectiveness of QGA, different optimizing methods were compared. The same training samples and test samples were selected. GA-MCMC-ARIMA and PSO-MCMC-ARIMA were used to predict wind power range and compared with the QGA-MCMC-ARIMA optimization model proposed in this paper. A comparison of performance indicators is presented in Table 3.

NAD is the normalized average deviation. The degree of bandwidth deviation of the prediction interval of the  $i$ -th iteration is

$$\varepsilon_i^\alpha = \begin{cases} \frac{L_t^\alpha(x_i) - t_i}{U_t^\alpha(x_i) - L_t^\alpha(x_i)}, & \text{if } t_i < L_t^\alpha(x_i) \\ 0, & \text{if } t_i \in I_t^\alpha(x_i) \\ \frac{t_i - U_t^\alpha(x_i)}{U_t^\alpha(x_i) - L_t^\alpha(x_i)}, & \text{if } t_i > U_t^\alpha(x_i) \end{cases} \quad (18)$$

The NAD of the prediction interval is

$$NAD_t^\alpha = \frac{1}{N} \sum_{i=1}^{N_t} \varepsilon_i^\alpha \quad (19)$$

**TABLE 3.** Performance indicators under different algorithms.

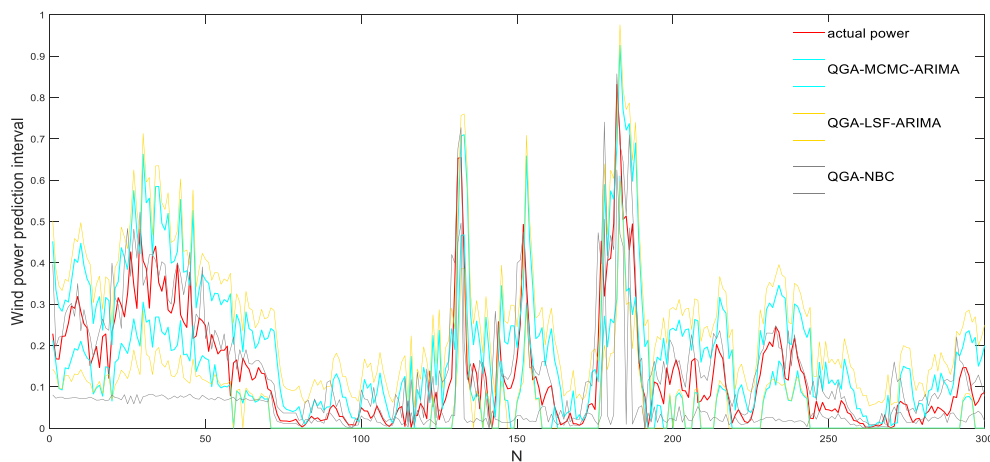
Confidence /%	Method	PICP/%	PINAW	NAD
80	GA	80.33	0.1352	0.0072
	PSO	80.67	0.1301	0.0025
	QGA	81.67	0.1304	0.0008
	GA	86.33	0.1542	0.0089
85	PSO	86.67	0.1547	0.0043
	QGA	87.00	0.1488	0.0011
	GA	90.00	0.1806	0.0134
	PSO	90.33	0.1805	0.0078
90	QGA	90.67	0.1760	0.0026

NAD represents the accumulation of target values that fall outside the interval according to the degree of deviation. The smaller the NAD value, the higher the quality of the prediction interval.

Under each confidence level,  $PICP_{QGA} > PICP_{PSO} > PICP_{GA}$ , and the average interval of the prediction interval

**TABLE 4.** Performance indicators under different algorithms.

Confidence /%	Method	PICP/%	PINAW	NAD
80	QGA-NBC	75.33	0.1193	0.0023
	QGA-LSF-ARIMA	81.33	0.1400	0.0025
	QGA-MCMC-ARIMA	81.67	0.1304	0.0008
85	QGA-NBC	80.67	0.1556	0.0030
	QGA-LSF-ARIMA	86.67	0.1632	0.0034
	QGA-MCMC-ARIMA	87.00	0.1488	0.0011
90	QGA-NBC	86.00	0.2018	0.0039
	QGA-LSF-ARIMA	89.00	0.1942	0.0036
	QGA-MCMC-ARIMA	90.67	0.1760	0.0026

**FIGURE 10.** Three methods of wind power interval prediction based on QGA algorithm.

of the QGA method was smallest under the same confidence level; a smaller interval average bandwidth denotes higher prediction accuracy and a smaller degree of uncertainty. At the same time, NAD was the smallest in the QGA method. On the basis of this comprehensive comparison, the QGA method can obtain better prediction results.

In order to verify the effectiveness of MCMC-ARIMA, an ARIMA parameter model estimated by the least squares fit (LSF-ARIMA) and a naive Bayes model (NBC) were carried out for comparison and analysis. Fig. 10 shows the wind power prediction interval based on the QGA algorithm by the above method, and its performance indicators are shown in Table 4.

Under each confidence level,  $PICP_{QGA-MCMC-ARIMA} > PICP_{QGA-LSF-ARIMA} > PICP_{QGA-NBC}$ , and under the same confidence level, the QGA-MCMC-ARIMA method has the smallest average prediction interval bandwidth and normalized average deviation, which shows that it has the highest accuracy.

On the basis of this comprehensive comparison, the QGA-MCMC-ARIMA method proposed in the paper can obtain better prediction results.

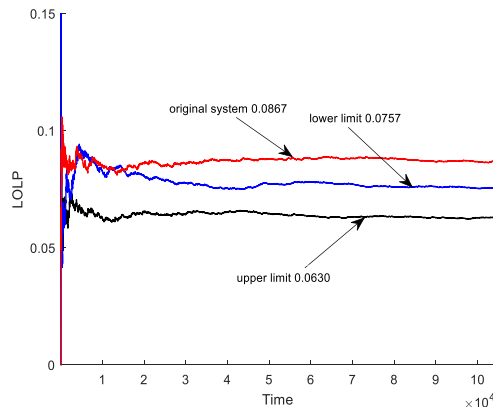
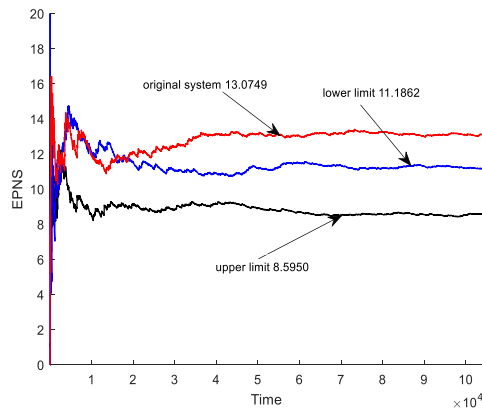
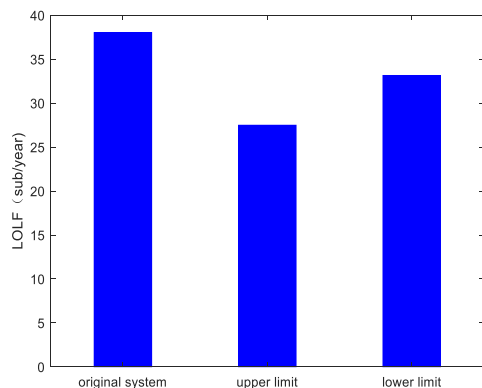
## B. RELIABILITY INDEX CALCULATION EXAMPLE RESULTS

This example uses the IEEE-RTS79 system, which contains 24 nodes, 71 components, 32 generators, 33 lines, and a

generator capacity of 12-400 MW. The annual peak load is 2850 MW, and the total installed capacity is 3405 MW [27]. The wind farm is connected to the system, and the access scheme refers to the distributed access method of [28]. In IEEE-RTS79 system, the wind power capacities 600 MW are integrated, where the connected nodes are node 13, node 15 and node 18 and installed capacity for every node is 200MW.

Using the sequential Monte Carlo method, the values of the reliability indicators LOLP, EPNS, and LOLF are calculated according to the flow chart in Fig. 3. To ensure minimum error in the Monte Carlo calculation, the simulation time is 400 years; thus, the calculated reliability index can converge completely. Figs. 11-13 depict a comparison of system reliability indices before and after the access system when the wind farm output is the upper limit and lower limit of the interval under the 85% confidence level. Table 5 shows reliability indicators at 80%, 85%, and 90% confidence levels.

The simulation results indicate that the addition of wind farms in the original RTS-79 node system can decrease system load loss frequency and load loss expectations. Taking the reliability index LOLP at the 85% confidence level as an example, when the wind farm output takes the upper-limit condition, the system LOLP value is at least 0.0630, 27.3% lower than the original system. The value at this time is recorded as the photovoltaic power station. When the working

**FIGURE 11.** Convergence curve of LOLP index.**FIGURE 12.** Convergence curve of EPNS index.**FIGURE 13.** LOLF of generation system.

condition is the lower limit of wind farm output, the LOLP value is 0.0757, (i.e., the LOLP value of the system is 12.7% lower than that of the original system). The value at this time is recorded as the lower limit of the LOLP of the wind farm. Wind farm output exhibited uncertainty. Overall, the system reliability ranges between 12.7% and 27.3%, implying a system reliability improvement of 12.7-27.3% after accessing the wind farm. The above reliability index calculation method provides a range that contributes to the reliability of the power grid after considering wind farm access, which offers guidance for wind farm planning, plan output adjustment, and power dispatch.

**TABLE 5.** Comparison of reliability index about generation system.

	LOLP/Decline	EPNS/ Decline	LOLF/ Decline
Original system	0.0867	13.0749	38.0347
Upper limit	80	0.0752/13.26%	10.5740/19.13%
	85	0.0630/27.34%	8.5950/34.26%
	90	0.0611/29.53%	8.4506/35.37%
Lower limit	80	0.0766/11.65%	11.1885/14.43%
	85	0.0757/12.69%	11.1862/14.45%
	90	0.0833/3.92%	11.8690/9.22%
			36.0096/5.32%

## VI. SUMMARY

In this paper, considering the uncertainty of wind power, the reliability indices of the grid connection are presented with probabilistic prediction interval model of wind power. The variation range of three system reliability indices can be obtained. Combining the MCMC-optimized Bayesian estimation ARIMA based on QGA is used to predict wind power. Our findings reveal the following:

(1) Through a reliability test system built, the impact integrated wind power to grid on system reliability index is analyzed: compared with the original system, whether the predicted power upper bound or lower bound is used, the three values of the reliability indicators LOLP, EPNS, and LOLF exhibit significant declines.

(2) We apply the limitation calculation method of the wind farm affecting the system reliability as shown in Section 4.2, to obtain the improvement range of system reliability under each confidence level. It provides a variable range of reliability index to power grid considering wind farm access, and thus carries reference significance with uncertainty information for planning a wind farm, adjusting the plan output, and guiding power dispatch.

(3) The wind power output probability interval is obtained by the MCMC-based Bayesian estimation ARIMA method, which utilizes prior knowledge and the distribution hypothesis of known data, and to assess Observed data based on these probabilities and distributions. Use reasoning to make the best judgment. The QGA optimization algorithm can be used to determine the best output weight for each power, leading to higher interval coverage and an obtained narrower bandwidth. Compared with the GA optimization method and PSO, the superior prediction effect of the proposed method is demonstrated.

## REFERENCES

- [1] K. Hou, X. Xu, H. Jia, X. Yu, T. Jiang, K. Zhang, and B. Shu, "A reliability assessment approach for integrated transportation and electrical power systems incorporating electric vehicles," *IEEE Trans. Smart Grid*, vol. 9, no. 1, pp. 88–100, Jan. 2018, doi: 10.1109/tsg.2016.2545113.
- [2] H.-Z. Wang, G.-Q. Li, G.-B. Wang, J.-C. Peng, H. Jiang, and Y.-T. Liu, "Deep learning based ensemble approach for probabilistic wind power forecasting," *Appl. Energy*, vol. 188, pp. 56–70, Feb. 2017, doi: 10.1016/j.apenergy.2016.11.111.

- [3] A. Khosravi and S. Nahavandi, "Combined nonparametric prediction intervals for wind power generation," *IEEE Trans. Sustain. Energy*, vol. 4, no. 4, pp. 849–856, Oct. 2013, doi: [10.1109/tste.2013.2253140](https://doi.org/10.1109/tste.2013.2253140).
- [4] J. Shi, J. Guo, and S. Zheng, "Evaluation of hybrid forecasting approaches for wind speed and power generation time series," *Renew. Sustain. Energy Rev.*, vol. 16, no. 5, pp. 3471–3480, Jun. 2012, doi: [10.1016/j.rser.2012.02.044](https://doi.org/10.1016/j.rser.2012.02.044).
- [5] F. Cassola and M. Burlando, "Wind speed and wind energy forecast through Kalman filtering of Numerical Weather Prediction model output," *Appl. Energy*, vol. 99, pp. 154–166, Nov. 2012, doi: [10.1016/j.apenergy.2012.03.054](https://doi.org/10.1016/j.apenergy.2012.03.054).
- [6] H. Liu, E. Erdem, and J. Shi, "Comprehensive evaluation of ARMA-GARCH-(M) approaches for modeling the mean and volatility of wind speed," *Appl. Energy*, vol. 88, no. 3, pp. 724–732, Mar. 2011, doi: [10.1016/j.apenergy.2010.09.028](https://doi.org/10.1016/j.apenergy.2010.09.028).
- [7] R. G. Kavasseri and K. Seetharaman, "Day-ahead wind speed forecasting using f-ARIMA models," *Renew. Energy*, vol. 34, no. 5, pp. 1388–1393, May 2009, doi: [10.1016/j.renene.2008.09.006](https://doi.org/10.1016/j.renene.2008.09.006).
- [8] G. Li and J. Shi, "On comparing three artificial neural networks for wind speed forecasting," *Appl. Energy*, vol. 87, no. 7, pp. 2313–2320, Jul. 2010, doi: [10.1016/j.apenergy.2009.12.013](https://doi.org/10.1016/j.apenergy.2009.12.013).
- [9] Y.-Y. Hong, H.-L. Chang, and C.-S. Chiu, "Hour-ahead wind power and speed forecasting using simultaneous perturbation stochastic approximation (SPSA) algorithm and neural network with fuzzy inputs," *Energy*, vol. 35, no. 9, pp. 3870–3876, Sep. 2010, doi: [10.1016/j.energy.2010.05.041](https://doi.org/10.1016/j.energy.2010.05.041).
- [10] H. Liu, H.-Q. Tian, D.-F. Pan, and Y.-F. Li, "Forecasting models for wind speed using wavelet, wavelet packet, time series and artificial neural networks," *Appl. Energy*, vol. 107, pp. 191–208, Jul. 2013, doi: [10.1016/j.apenergy.2013.02.002](https://doi.org/10.1016/j.apenergy.2013.02.002).
- [11] J. Zhou, J. Shi, and G. Li, "Fine tuning support vector machines for short-term wind speed forecasting," *Energy Convers. Manage.*, vol. 52, no. 4, pp. 1990–1998, Apr. 2011, doi: [10.1016/j.enconman.2010.11.007](https://doi.org/10.1016/j.enconman.2010.11.007).
- [12] J. B. Bremnes, "Probabilistic wind power forecasts using local quantile regression," *Wind Energy*, vol. 7, no. 1, pp. 47–54, Jan. 2004, doi: [10.1002/we.107](https://doi.org/10.1002/we.107).
- [13] C. Tian, Y. Hao, and J. Hu, "A novel wind speed forecasting system based on hybrid data preprocessing and multi-objective optimization," *Appl. Energy*, vol. 231, pp. 301–319, Dec. 2018, doi: [10.1016/j.apenergy.2018.09.012](https://doi.org/10.1016/j.apenergy.2018.09.012).
- [14] R. Jiao, X. Huang, X. Ma, L. Han, and W. Tian, "A model combining stacked auto encoder and back propagation algorithm for short-term wind power forecasting," *IEEE Access*, vol. 6, pp. 17851–17858, 2018, doi: [10.1109/access.2018.2818108](https://doi.org/10.1109/access.2018.2818108).
- [15] F. Ge, Y. Ju, Z. Qi, and Y. Lin, "Parameter estimation of a Gaussian mixture model for wind power forecast error by Riemann L-BFGS optimization," *IEEE Access*, vol. 6, pp. 38892–38899, 2018, doi: [10.1109/access.2018.2852501](https://doi.org/10.1109/access.2018.2852501).
- [16] W. Wu, Y. Qiao, Z. Lu, N. Wang, and Q. Zhou, "Methods and prospects for probabilistic forecasting of wind power," *Automat. Electr. Power Syst.*, vol. 41, no. 18, pp. 167–175, Sep. 2017, doi: [10.7500/AEPS20160914002](https://doi.org/10.7500/AEPS20160914002).
- [17] Y. Zhang, K. Liu, L. Qin, and X. An, "Deterministic and probabilistic interval prediction for short-term wind power generation based on variational mode decomposition and machine learning methods," *Energy Convers. Manage.*, vol. 112, pp. 208–219, Mar. 2016, doi: [10.1016/j.enconman.2016.01.023](https://doi.org/10.1016/j.enconman.2016.01.023).
- [18] M. Hu, Z. Hu, J. Yue, M. Zhang, and M. Hu, "A novel multi-objective optimal approach for wind power interval prediction," *Energies*, vol. 10, no. 4, p. 419, Mar. 2017, doi: [10.3390/en10040419](https://doi.org/10.3390/en10040419).
- [19] S. Shi and K. L. Lo, "Reliability assessment of power system considering the impact of wind energy," in *Proc. 47th Int. Univ. Power Eng. Conf. (UPEC)*, Sep. 2012, doi: [10.1109/upec.2012.6398666](https://doi.org/10.1109/upec.2012.6398666).
- [20] F. Cao, X. Gao, and J. Yu, "Study on reliability assessment of composite generation and transmission system integrated wind farm," in *Proc. IEEE Int. Conf. Power System Technol. (POWERCON)*, Oct. 2012, doi: [10.1109/powercon.2012.6401359](https://doi.org/10.1109/powercon.2012.6401359).
- [21] F. Vallee, J. Lobry, and O. Deblecker, "Impact of the wind geographical correlation level for reliability studies," *IEEE Trans. Power Syst.*, vol. 22, no. 4, pp. 2232–2239, Nov. 2007, doi: [10.1109/tpwrs.2007.907969](https://doi.org/10.1109/tpwrs.2007.907969).
- [22] W. Li, J. Zhou, J. Lu, and W. Yan, "Incorporating a combined fuzzy and probabilistic load model in power system reliability assessment," *IEEE Trans. Power Syst.*, vol. 22, no. 3, pp. 1386–1388, Aug. 2007, doi: [10.1109/tpwrs.2007.901676](https://doi.org/10.1109/tpwrs.2007.901676).
- [23] F. Cadini, G. L. Agliardi, and E. Zio, "A modeling and simulation framework for the reliability/availability assessment of a power transmission grid subject to cascading failures under extreme weather conditions," *Appl. Energy*, vol. 185, pp. 267–279, Jan. 2017, doi: [10.1016/j.apenergy.2016.10.086](https://doi.org/10.1016/j.apenergy.2016.10.086).
- [24] S.-S. Shi, *Bayesian Statistics*. Beijing, China: China Statistics Press, 1999, pp. 16–64.
- [25] X. W. Wang, J. H. Zhang, C. Jiang, and L. Yu, "Probabilistic assessment of wind farm active power based on monte-carlo simulation," *Appl. Mech. Mater.*, vols. 291–294, pp. 536–540, Mar. 2013, doi: [10.4028/www.scientific.net/amm.291-294.536](https://doi.org/10.4028/www.scientific.net/amm.291-294.536).
- [26] Y. Wang, K. Xie, and B. Hu, "Reliability analysis of islanded microgrid based on sequential simulation," *Trans. China Electrotech. Soc.*, vol. 31, no. 6, pp. 206–211, Mar. 2016, doi: [10.19595/j.cnki.1000-6753.tces.2016.06.023](https://doi.org/10.19595/j.cnki.1000-6753.tces.2016.06.023).
- [27] P. Subcommittee, "IEEE reliability test system," *IEEE Trans. Power App. Syst.*, vol. PAS-98, no. 6, pp. 2047–2054, Nov. 1979, doi: [10.1109/tpas.1979.319398](https://doi.org/10.1109/tpas.1979.319398).
- [28] S. Zhang, "Reliability studies of power systems concerning capacity credit of wind farms," Ph.D. dissertation, Dept. Elect. Eng., North China Electr. Power Univ., Beijing, China, 2010.

**XIYUN YANG** received the Ph.D. degree from North China Electric Power University, Beijing, China, in 2004.



She is currently a Professor with the School of Control and Computer Engineering, North China Electric Power University. Her research interests include renewable energy, energy analytics, smart power systems, and electricity markets.

**YUWEI YANG** received the bachelor's degree from Shanxi University, Taiyuan, China, in 2018. She is currently pursuing master's degree with the School of Control and Computer Engineering, North China Electric Power University.



Her research interests include renewable energy, wind power forecasting, and power system reliability analysis.

**YUQI LIU** received the master's degree from North China Electric Power University, Beijing, China, in 2017.



He is currently working with the Shenyang Institute of Automation, Chinese Academy of Sciences.

**ZIQI DENG** received the bachelor's degree from North China Electric Power University, Beijing, China, in 2019, where she is currently pursuing master's degree with the School of Control and Computer Engineering.



Her research interests are renewable energy and wind power forecasting.